FEASIBILITY STUDY OF A SYNTHESIS PROCEDURE FOR ARRAY FEEDS TO IMPROVE RADIATION PERFORMANCE OF LARGE DISTORTED REFLECTOR ANTENNAS

Grant No. NAG-1-859

FINAL REPORT
covering the period
February 25, 1988 to February 24,1989.

by

W. L. Stutzman
W. T. Smith
Bradley Department of Electrical Engineering
Virginia Polytechnic Institute and State University
Blacksburg, VA 24061

INTRODUCTION

Surface errors on parabolic reflector antennas degrade the overall performance of the antenna. The errors are in the form of roughness on the surface, distortions in the shape, or structural design details (such as ribbing, slots between panels, etc.). They cause amplitude and phase errors in the aperture field which lower the gain, raise the side lobes, and fill in the nulls. These are major problems in large space reflector antenna systems. Planned mobile satellite communications systems having limited signal margin need high gain from the space reflectors. Future multiple beam antenna systems requiring spatial isolation to allow frequency reuse could be rendered useless if high side lobes are present. High side lobes are also responsible for noise. This is especially troublesome for radiometric systems such as in remote sensing applications.

Electromagnetic compensation for surface errors in large space reflector antennas has been the topic of several research studies. Most of these studies try to correct the focal plane fields of the reflector near the focal point and, hence, compensate for the distortions in the overall radiation pattern. This study examines ways of compensating for surface errors by pattern synthesis using an array of feed antennas. It differs from previous approaches in that pattern corrections are directed specifically toward portions of the pattern requiring improvements. The pattern synthesis approach does not require knowledge of the surface errors.

WORK SUMMARY

Work was divided nearly equally between documentation and computation. First, we performed a comprehensive literature survey. This was necessary because of the wealth of existing knowledge in related topics. Many pertinent papers were included in the survey.

Second, we studied parabolic reflectors using a computer code written for this project. The FORTRAN programs RAPCA (Reflector Analysis Program for Cylindrical Antennas) and SCANRAP (SCANned Reflector Analysis Program) were used extensively to compute radiation patterns for smooth and distorted parabolic cylinder reflectors. There are both physical and mathematical advantages to studying this class of problems. The radiation integral is a single integral and the associated fields are scalar, not vector. Greater physical insight is facilitated by the use of the simpler equations.

Some preliminary compensation cases using pattern synthesis were analyzed. The results showed that improvement in the radiation pattern is possible using pattern synthesis and encouraged further study into finding the best method for implementing the technique and extending the method to paraboloidal reflectors.

SCANNING STUDIES

The ability to scan the pattern of a reflector is essential to the proposed compensation method using pattern synthesis. Scanning is required to place a compensation beam (using an auxiliary feed) in the direction of an unwanted pattern lobe created by surface distortions. An extensive scan study was performed on a cylindrical reflector with $F/D = 0.4$, $D = 100\lambda$.

Feed Displacement

The ultimate design goal was to scan with a phased array feed; such electronic scanning is discussed below. Scanning was first implemented by moving the feed in the focal plane. The feed pattern was assumed to be a $\cos^q\theta$ pattern with $q = 3$. Patterns were computed by moving a single feed in the focal plane for cases of up to 4λ of lateral feed displacement. This produces scans of up to about 9 beamwidths. The patterns were calculated for smooth reflectors as well as distorted reflectors. The surface distortion

used sets up a surface error corresponding to a sinusoidal phase error in the equivalent PO aperture plane current.

The position function for the distorted cylindrical reflector surface is given by

$$z = \frac{x^2 - 2F\xi - \xi^2}{4F + 2\xi}$$

where x is the distance from the focal point along the radius, F is the focal length, and

$$\xi = \gamma \cos\left(\frac{4\pi m x}{D} \right)$$

where γ is the magnitude of the surface error (in wavelengths) and m is the number of periods along the radius of the reflector. This surface error determines the phase error in the aperture, ϕ_E, given by

$$\phi_E = \alpha \cos\left(\frac{4\pi m x}{D} \right)$$

where $\alpha = (2\pi/\lambda)\gamma$. The periodic nature of the surface error creates a region of high side lobes over an angular location determined by the spatial frequency (m) of the surface error.

Examples of unscanned smooth and distorted reflector patterns computed using RAPCA are shown in Fig. 1. Note that the pattern angle where the region of high side lobes occurs increases as the frequency of the phase error increases (m increases). Also, the amplitude of the side lobes increases with increasing amplitude of the phase error.

Scanning of the beam causes the side lobe envelope to rise and the gain to drop. Figures 2 and 3 show examples of scanned smooth and distorted reflector radiation patterns. Note that while the high side lobe regions caused by the surface distortions appear in nearly the same location relative to the main beam, the main beam is nearly unaffected by the surface distortions.

It is necessary to have the amplitude and phase information for the scanned beam in order to apply our proposed pattern synthesis compensation technique. The amplitudes and phases of the scanned beams produced by lateral displacement of the feed for the smooth and distorted reflector mentioned above were compared. The important point to be noted from the scan study is that, while the side lobe regions of the scanned patterns (Figs. 2 and 3) were noticeably affected by the surface distortion, the amplitudes and phases at the peak of the scanned beams for the distorted reflector do not vary greatly from the smooth reflector. This means that the amplitudes and phases of the auxiliary beams that will be used for compensation are essentially known based on smooth reflector performance. This is a major result because it implies that knowledge of the actual surface deviations is not required.

Electronic Scanning

The cylindrical scanning study concluded with examination of electronic scanning. Again, a 100λ cylindrical reflector with $F/D = 0.4$ was used. The feed was a 7-element linear array with 0.5λ element spacing, centered on the focal line, and orthogonal to it. The element pattern was chosen to be the same as the single element in the above laterally displaced feed analysis.

The excitations of the elements were computed with SCANRAP. The program SCANRAP uses the method of conjugate field match to derive the element amplitudes and phases required to scan to a given θ_0 . This is accomplished by computing the radiation integral to find the values of the focal plane field at the locations of the feed elements when a plane wave assumed to be incident from the θ_0 -direction. The excitations are the complex conjugates of the values of the received focal plane field at the feed element locations. Figure 4 shows examples of electronically scanned beams. Comparison to Figs. 2 and 3 reveals that the electronically scanned beams show improved side lobe envelope and gain loss performance compared to the single, laterally displaced feed. With the above 6λ-diameter feed array configuration, the reflector is

limited to about ± 3 beamwidths of scan. This limit could be increased by using a larger array.

As with the scanned beams using laterally displaced feeds, it was found that the amplitude and phase of the scanned beams for the distorted reflector using a phased array feed did not vary greatly from the smooth reflector. This means that for the electronic scanned case that the amplitudes and phases of the auxiliary beams used for compensation are essentially known.

PRELIMINARY COMPENSATION RESULTS

Compensation with Feed Displacement

Some preliminary compensation calculations were run for the $F/D = 0.4$, $D = 100\lambda$ distorted reflector corresponding to the pattern in Fig. 1(b). An auxiliary scanned beam produced by a second feed was used to null out the high side lobe caused by the surface distortion. The element pattern of the auxiliary feed was assumed to be the same as the feed at the focal point. The compensated pattern is shown in Fig. 5. This was accomplished by scanning the auxiliary beam to the location of the high side lobe, weighting the scanned beam so that it had equal amplitude and opposite phase to that of the side lobe peak. The amplitude and phase of the side lobe peak were obtained from computations on the distorted reflector using RAPCA. Normally this information is not available. A possible method of obtaining this information is discussed in the conclusions section below.

A reflector with $F/D = 1.0$ and $D = 100\lambda$ was also analyzed. The advantage of the higher F/D-ratio is less degradation in the side lobe envelope for a given scan angle. The disadvantage is that the lateral feed displacement increases for a given angle of scan. A composite of three scans is shown in Fig. 6. Compensation for the high side lobes was performed for the cases of $F/D = 1.0$ and 2.3° scan angle in Fig. 7 and 5.76° scan angle in Fig. 8. Again, a displaced feed was used to scan the auxiliary beam. The increased

scan range of this case allows compensation much further out than with the $F/D = 0.4$ case (the $F/D = 0.4$ case was limited to about a $\pm 3°$ compensation range).

Electronic Compensation with an Array Feed

Electronic compensation was performed on the distorted reflector corresponding to the pattern in Fig. 9. This distorted reflector has a slightly different surface error spatial frequency than the reflector from Fig. 1(b). The feed array was the same seven element array used previously. Auxiliary scanned beams given by Fig. 10 were simultaneously used to reduce the high side lobes caused by the surface distortion. The excitations for the scanned beams are computed assuming a smooth surface. In one case the auxiliary beams were weighted to produce a 10 dB reduction in the peak of the high side lobes (Fig. 11), and in a second case to place a null at the location of the peak of the high side lobes (Fig. 12). Comparing Figures 11 and 12, it is seen that not much advantage is gained by placing a null at the location of the high side lobes as opposed to just reducing the level significantly.

CONCLUSIONS

The pattern synthesis approach was shown to be a feasible method for electromagnetically compensating for surface errors in large reflectors. The method was demonstrated using cylindrical reflectors. The method can be extended to paraboloidal reflectors as well.

The advantage to using this approach is that knowledge of the surface errors is not required. It does require pattern data. Both the amplitude and phase of the high side lobes caused by the distortion are required.

The work will continue with extension of the method to paraboloidal reflectors. The improved scanning characteristics of the higher F/D reflector will prompt investigation into using a dual reflector configuration with a high F/D-ratio. In addition,

it looks feasible to derive the phase of the high side lobes by using amplitude measurements only. This vector amplitude approach will also be analyzed.

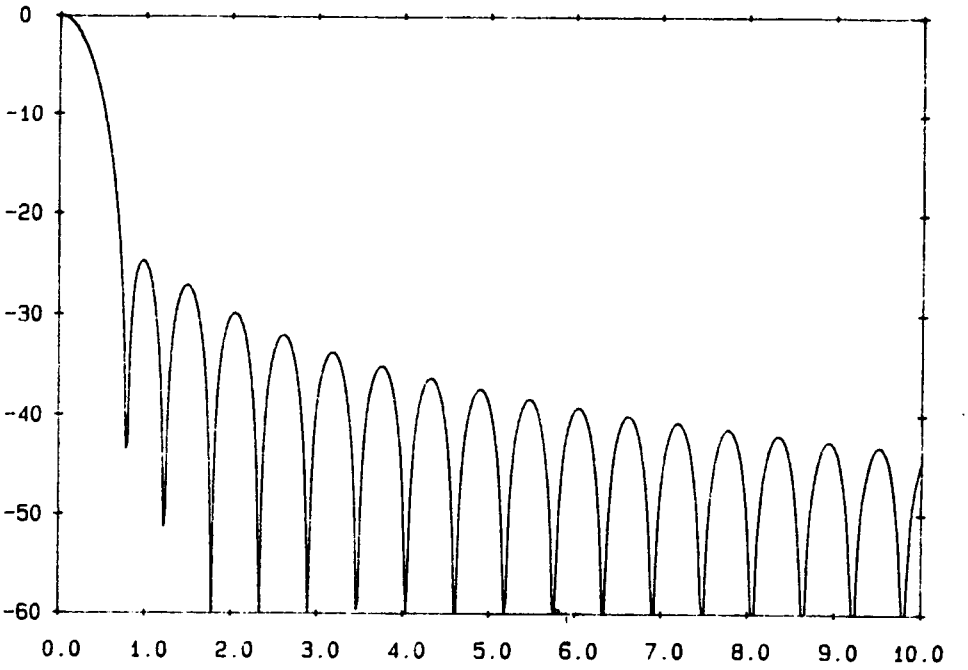

(a)

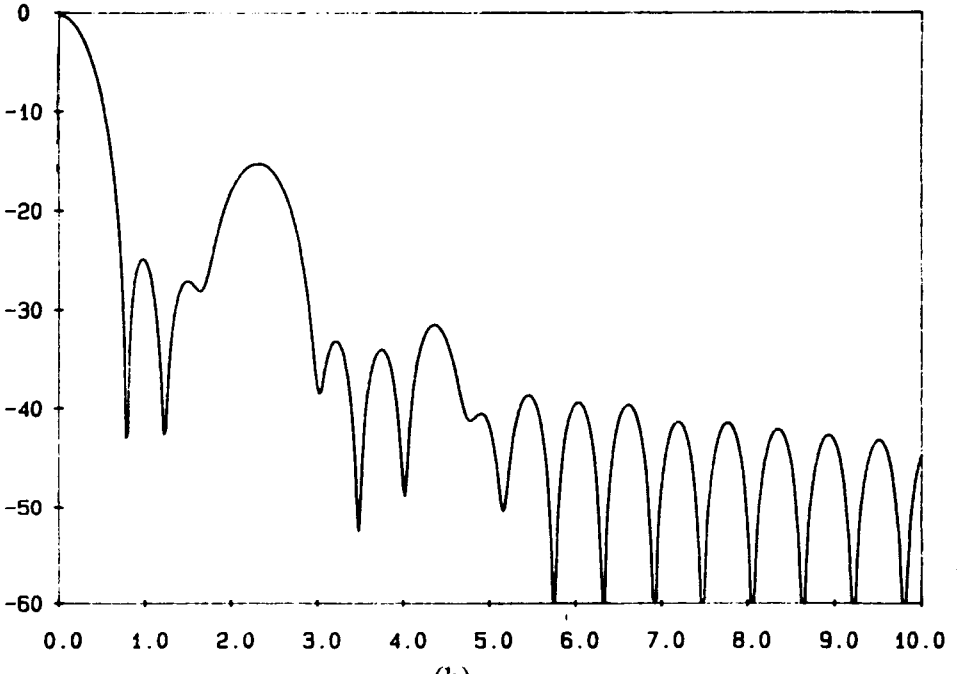

(b)

Figure 1. Unscanned beam for (a) smooth reflector, (b) distorted reflector with 2 periods of the surface error across the reflector, and (c) distorted reflector with 5 periods of the surface error across the reflector. The surface errors are such that a sinusoidal phase error appears across the aperture with a peak phase error of f.phi sub E = 20 degree . The *F*/*D* is 0.4.

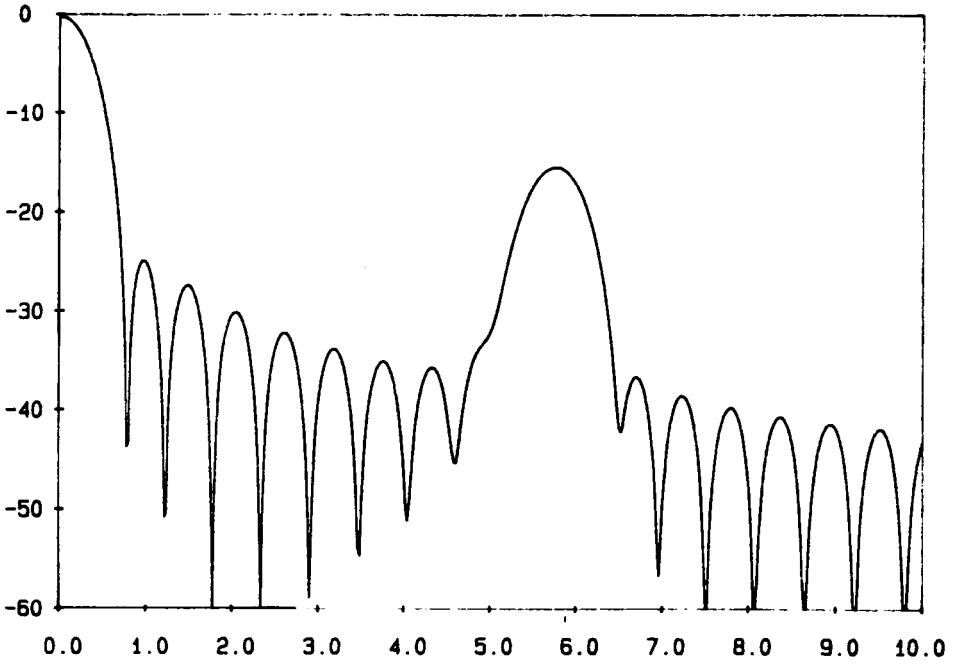

(c)

Figure 1. (continued)

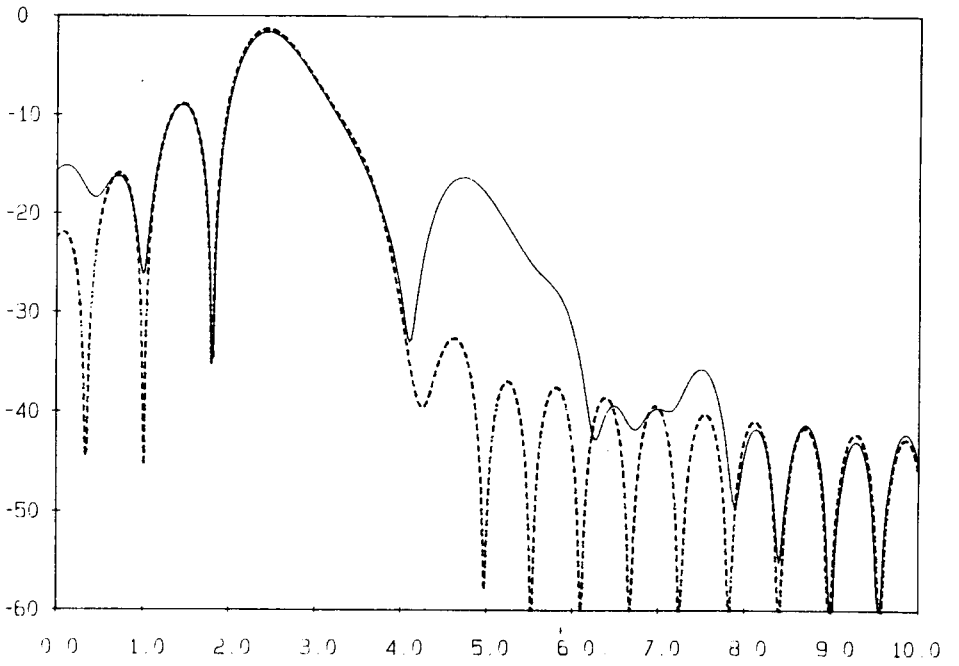

Figure 2. Scanned reflector patterns for lateral feed displacement of 2λ. The cases are for smooth reflector (dashed) and distorted reflector (solid) with 2 periods of the surface error across the reflector ($F/D = 0.4$).

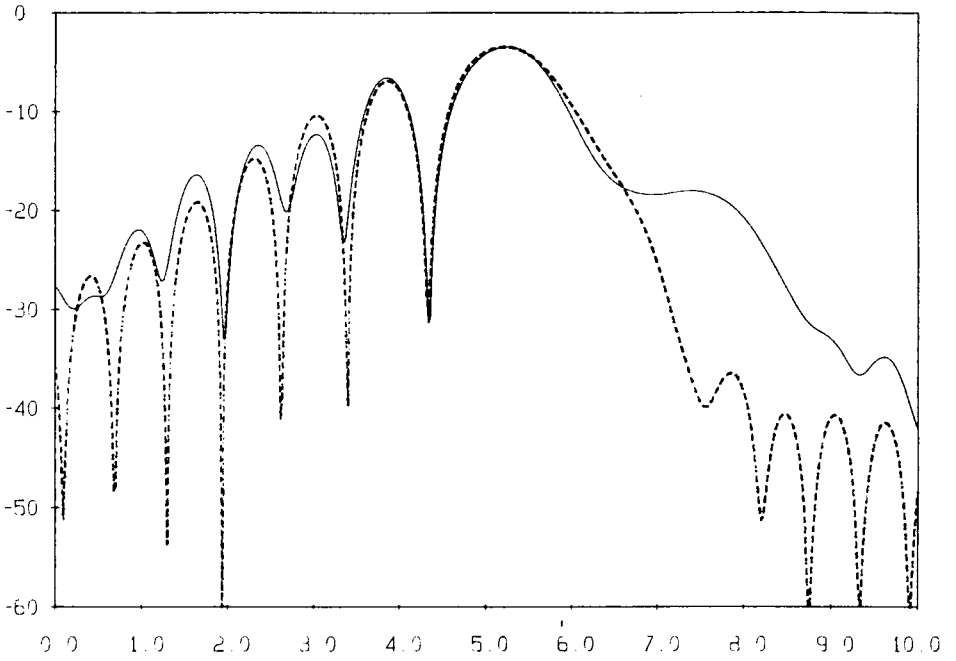

Figure 3. Scanned reflector patterns for lateral feed displacement of 4λ. The cases are for smooth reflector (dashed) and distorted reflector (solid) with 2 periods of the surface error across the reflector ($F/D = 0.4$). This beam is probably beyond the useful limit of our compensation technique as the side lobes are too high.

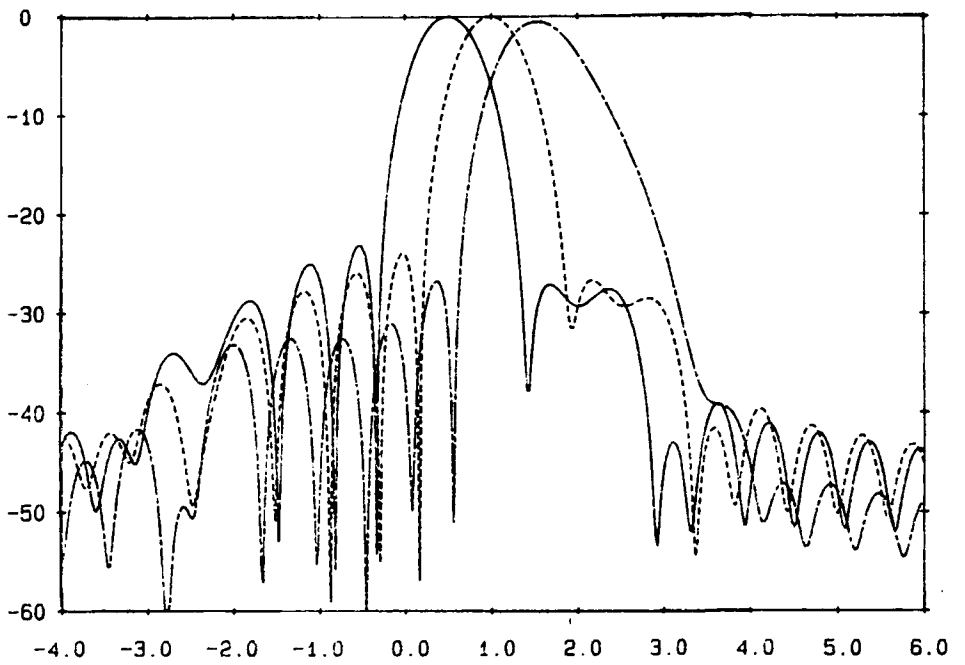

Figure 4. Electronically scanned beams for a cylindrical reflector with $F/D = 0.4$ and $D = 100\lambda$. A 7-element array feed with 0.5λ -element spacing was used. The element excitations were computed with SCANRAP.

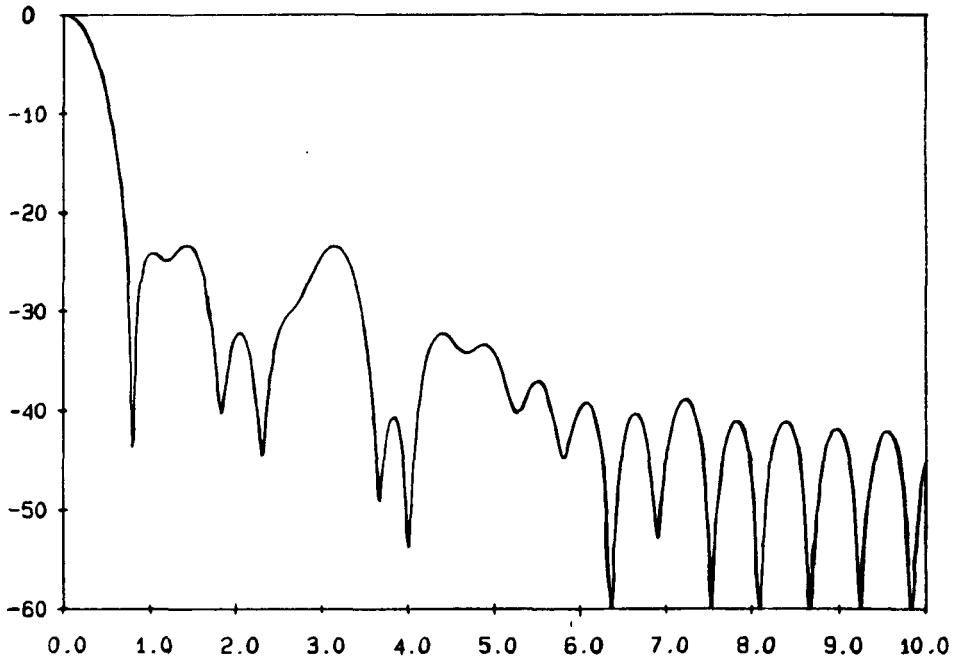

Figure 5. Compensation for the high side lobe at 2.3° of the distorted reflector in Fig. 1(b) using an auxiliary scanned beam generated by lateral displacement of a second feed ($F/D = 0.4$).

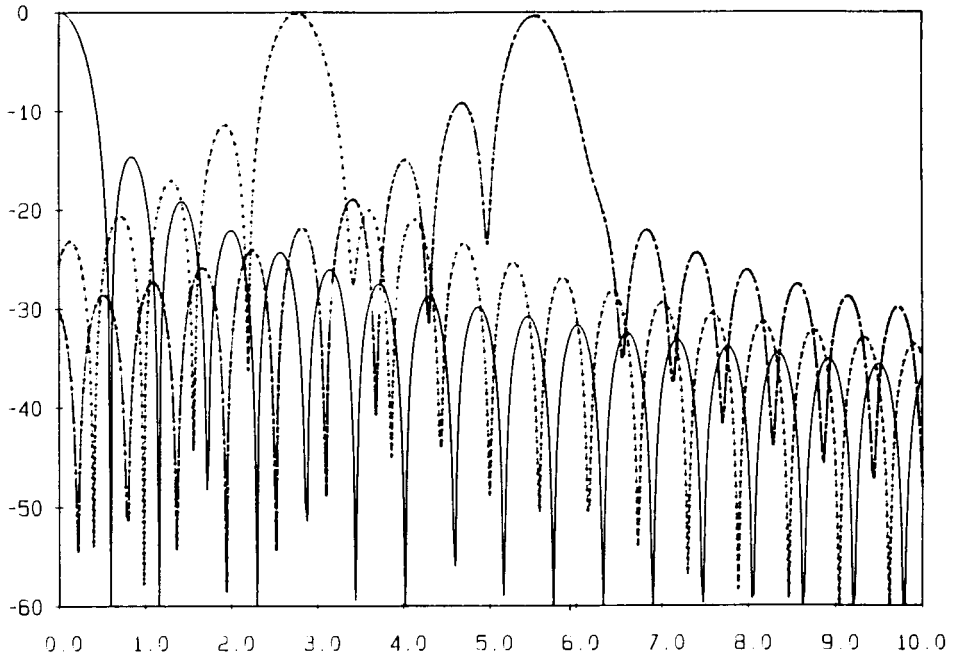

Figure 6. Radiation patterns for a smooth 100λ reflector with $F/D = 1.0$ for the cases of unscanned (solid), lateral feed displacement of 5λ (dashed), and lateral feed displacement of 10λ (nonuniformly dashed).

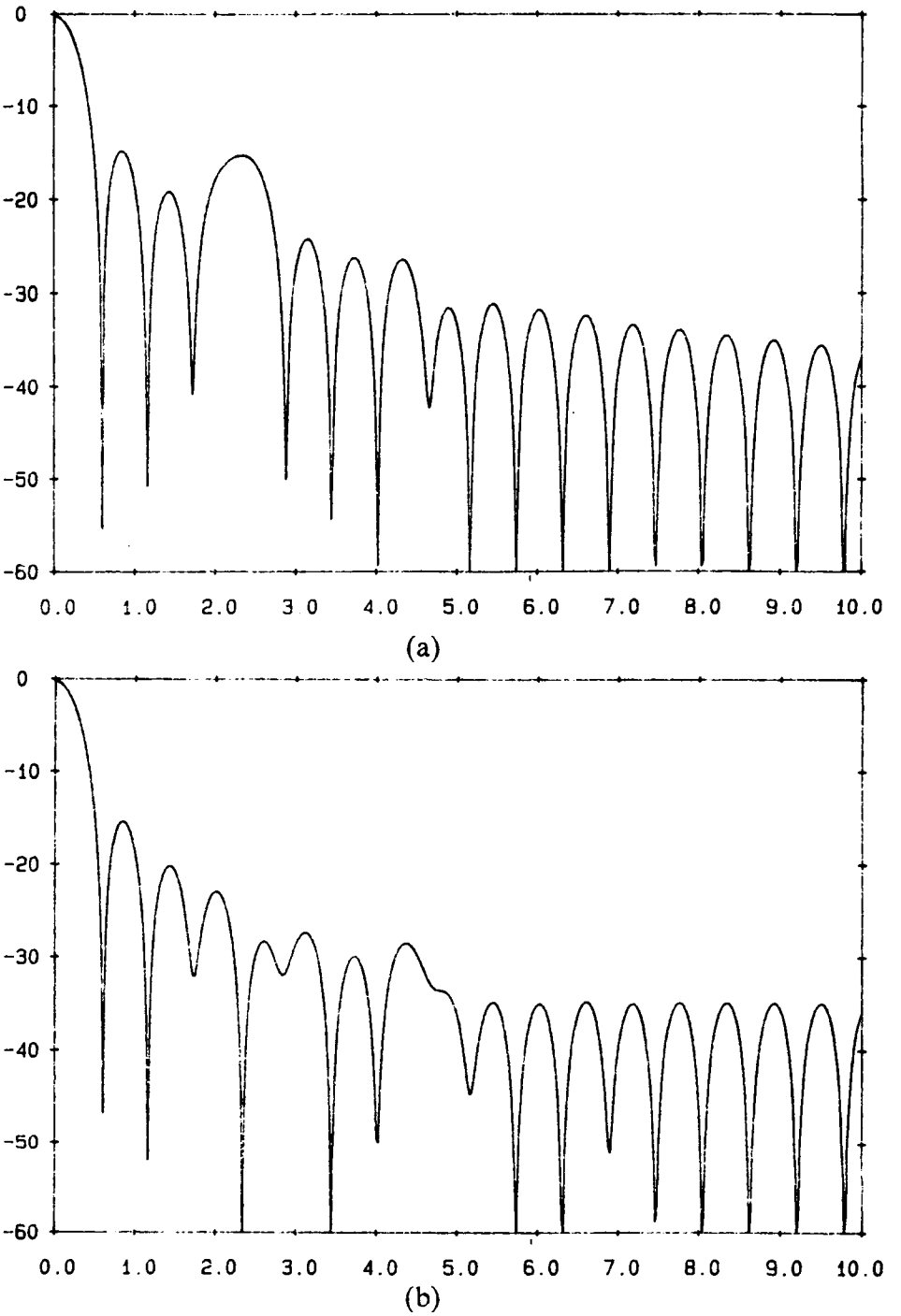

Figure 7. Radiation patterns for a distorted 100λ reflector with a distortion having two spatial periods, $F/D = 1.0$ for the cases of (a) uncompensated and (b) compensated. A second displaced feed was used to generate an auxiliary beam positioned at 2.3°.

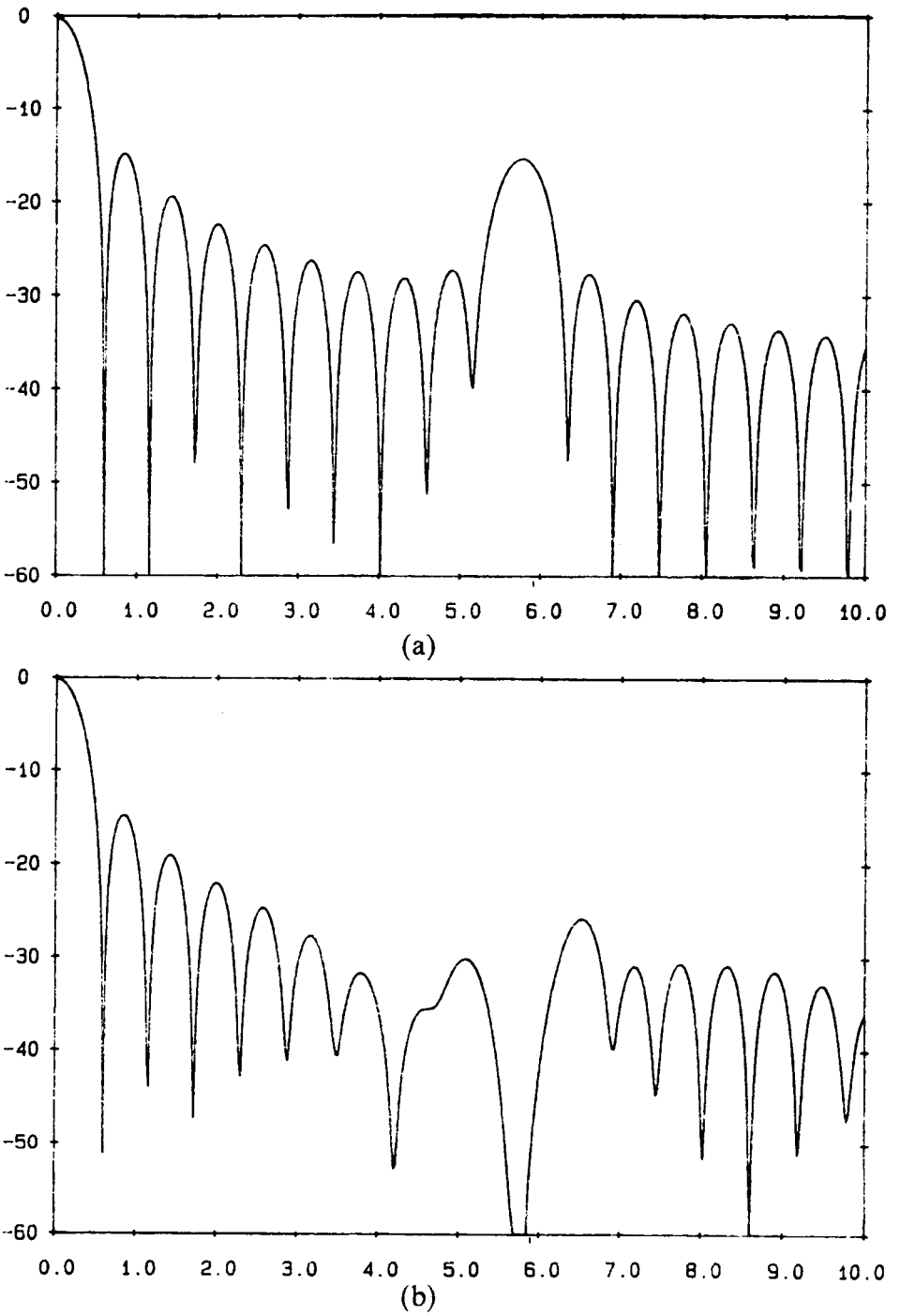

Figure 8. Radiation patterns for a distorted 100λ reflector with a distortion having five spatial periods, $F/D = 1.0$ for the cases of (a) uncompensated and (b) compensated. A second displaced feed was used to generate an auxiliary beam positioned at 5.76°.

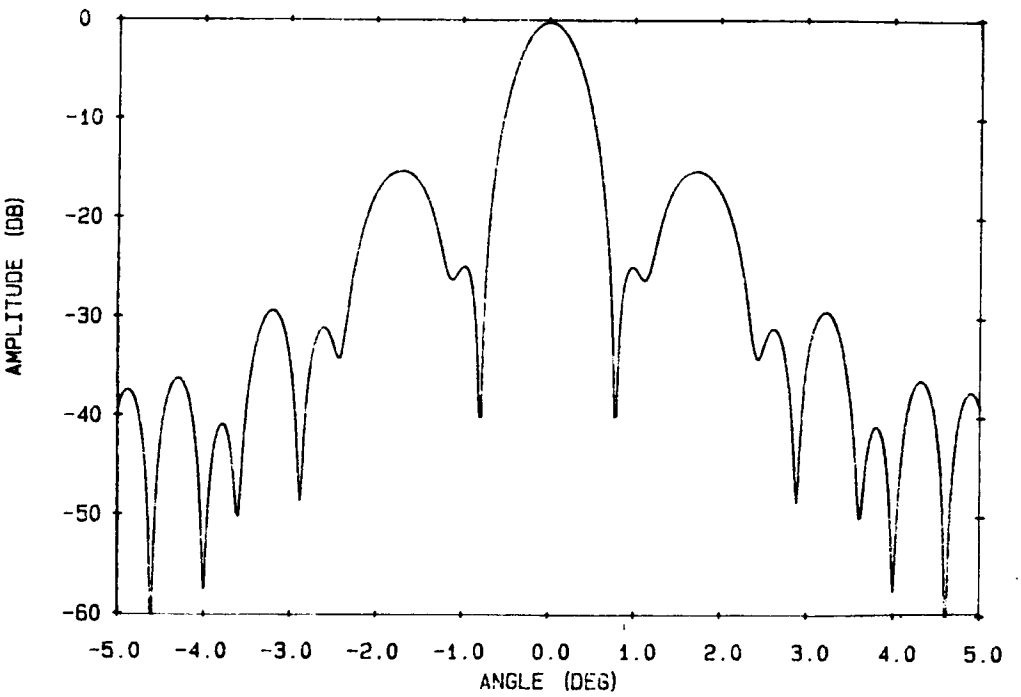

Figure 9. Unscanned beam for a distorted reflector with 1.5 periods of the surface error across the reflector. The $F/D = 0.4$ and $D = 100\lambda$. The max phase error in the PO current is $\phi_E = 20°$.

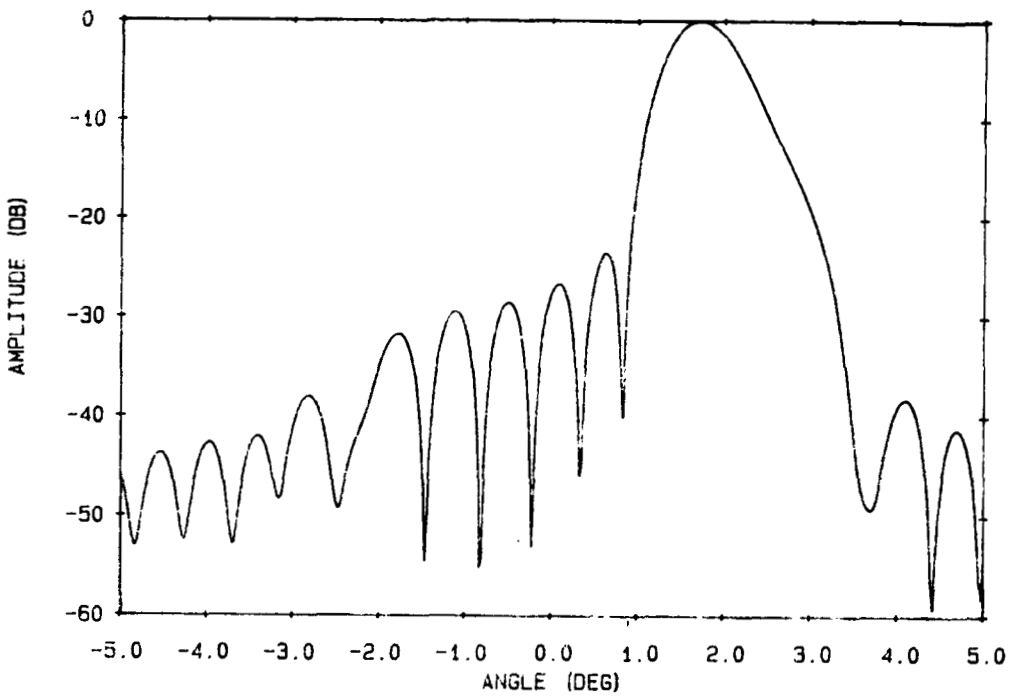

Figure 10. Auxiliary electronic scanned beam from a linear feed array of seven $\lambda/2$-spaced elements used to reduce the high side lobe at 1.72° caused by the surface error across the reflector of Fig. 9. The pattern was computed assuming a smooth reflector. A similar beam is used to reduce the high side lobe at -1.72°.

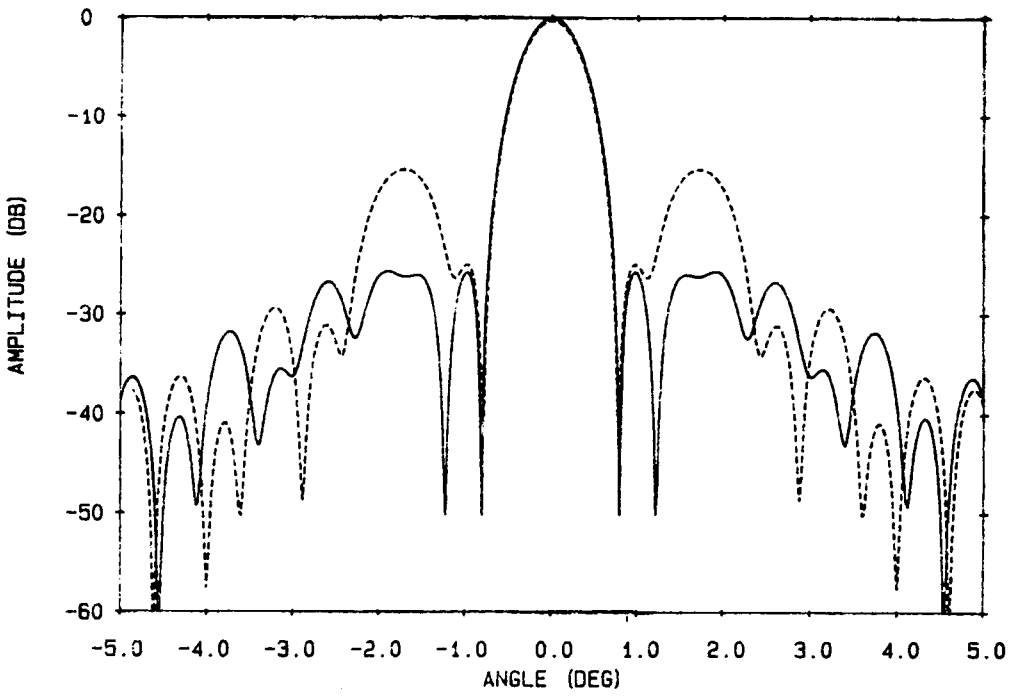

Figure 11. The pattern resulting from application of compensation for the high side lobes at $\pm 1.72°$ using the auxiliary scanned beams of Fig. 10 produced by a linear feed array of seven $\lambda/2$-spaced elements. The dashed line is the uncompensated pattern and the solid line is the compensated pattern. The amplitude of the weights were designed to produce a 10 dB reduction in the side lobe.

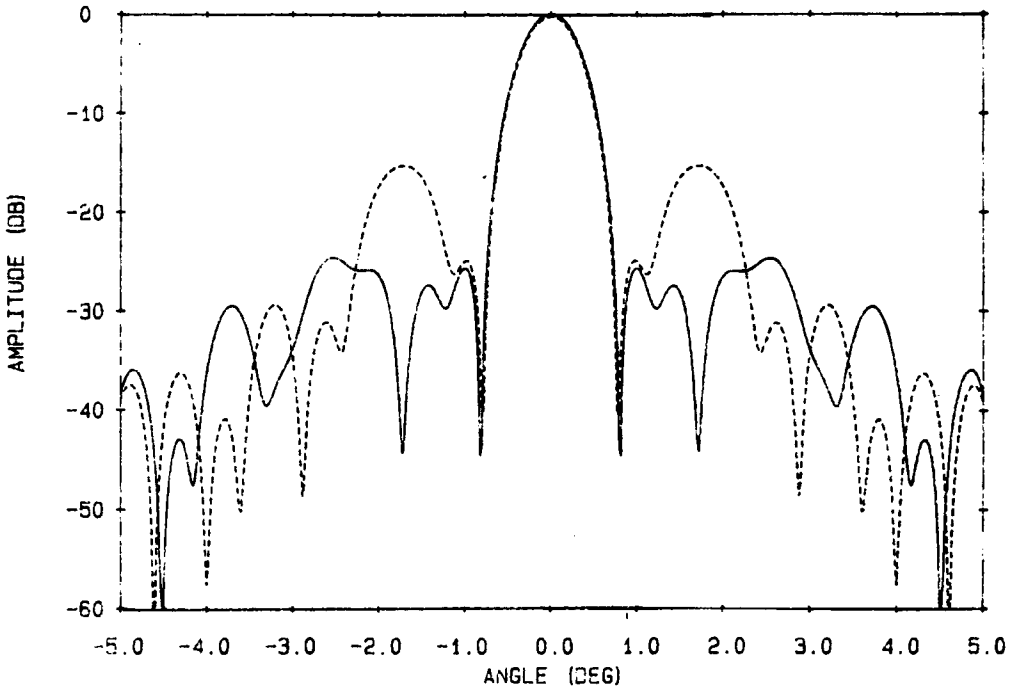

Figure 12. The pattern resulting from application of compensation for the high side lobes at $\pm 1.72°$ using the auxiliary scanned beams of Fig. 10 produced by a linear feed array of seven $\lambda/2$-spaced elements. The dashed line is the uncompensated pattern and the solid line is the compensated pattern. The amplitude of the weights were designed to produce a null at the peak of the side lobe.